SUPPORTING INFORMATION

Chinese Journal of Structural Chemistry

An Advanced Design Concept of Mansion-like Freestanding Silicon Anodes with Improved Lithium Storage Performances

Deqing Zhang[1,2], Junfeng Ren[1,2], Caixia Li[1,3]*, Bin Luo[4]*, Lei Wang[1,3]* and Yanyan Li[1]

[1]*State Key Laboratory Base of Eco-chemical Engineering, Taishan Scholar Advantage and Characteristic Discipline Team of Eco-chemical Process and Technology, Qingdao University of Science and Technology, Qingdao 266042, China*

[2]*College of Chemical Engineering, Qingdao University of Science and Technology, Qingdao 266042, China*

[3]*College of Environment and Safety Engineering, Qingdao University of Science and Technology, Qingdao 266042, China*

[4]*Nanomaterials Centre, School of Chemical Engineering and Australian Institute for Bioengineering and Nanotechnology, The University of Queensland, St Lucia, QLD 4072, Australia*

Corresponding author. E-mails: licaixia91@126.com (C. Li), b.luo1@uq.edu.au (B. Luo), inorchemwl@126.com (L. Wang)

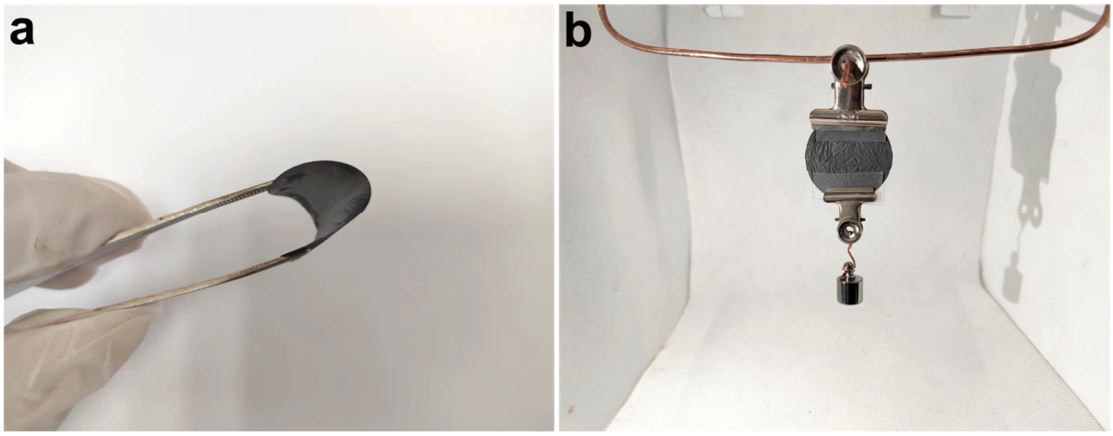

Figure S1. Mechanical properties test of SSPBG electrode

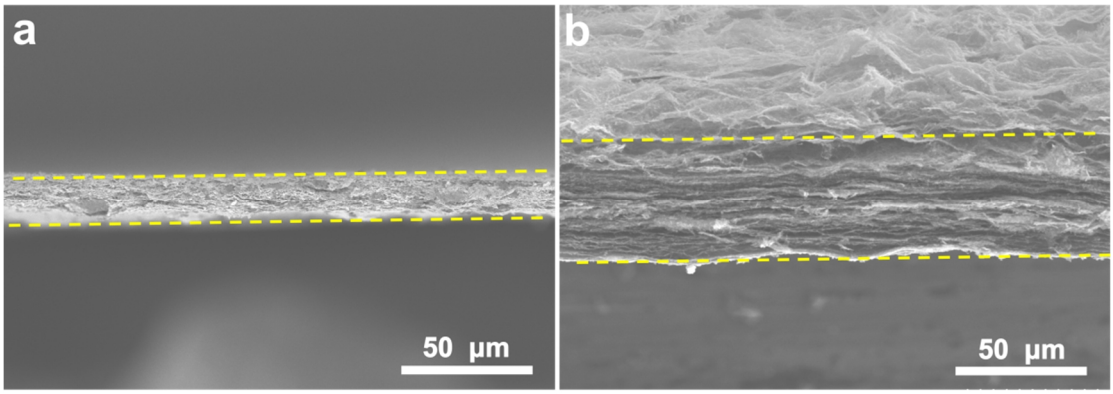

Figure S2. Cross-sectional SEM images of SSPBG with controllable thickness.

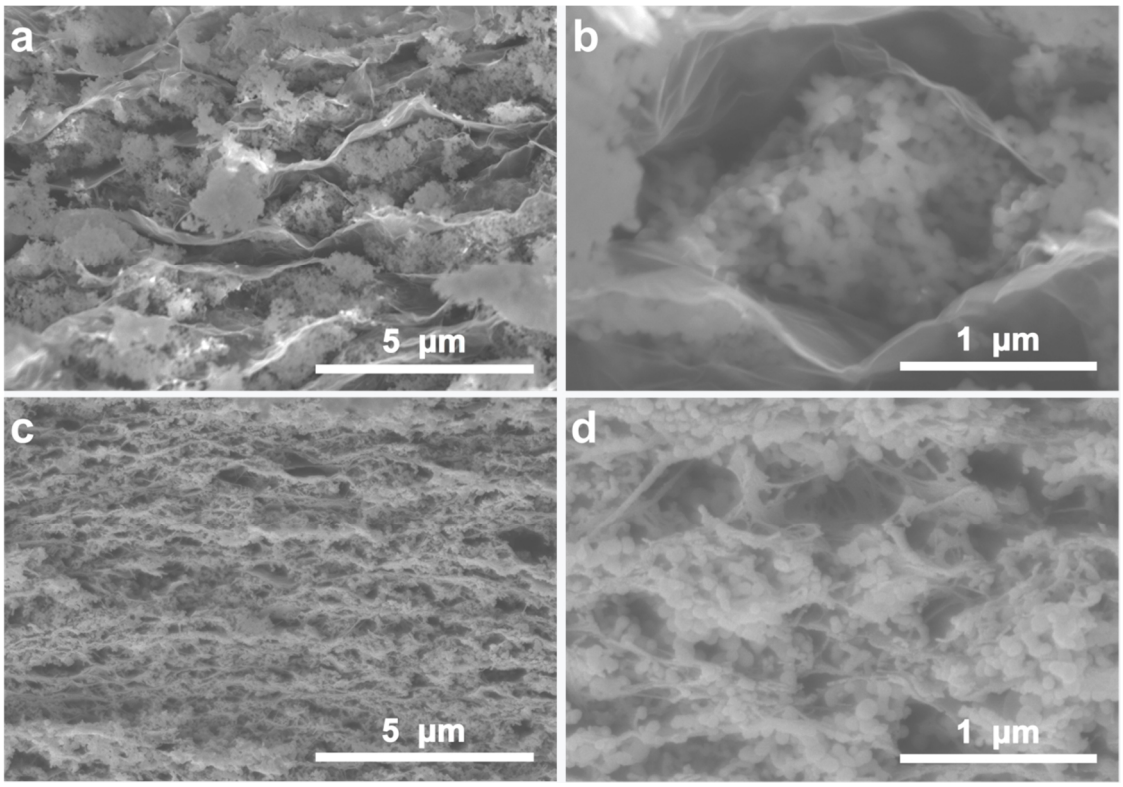

Figure S3. Cross-sectional SEM images of (a-b) SSG and (c-d) SSPB.

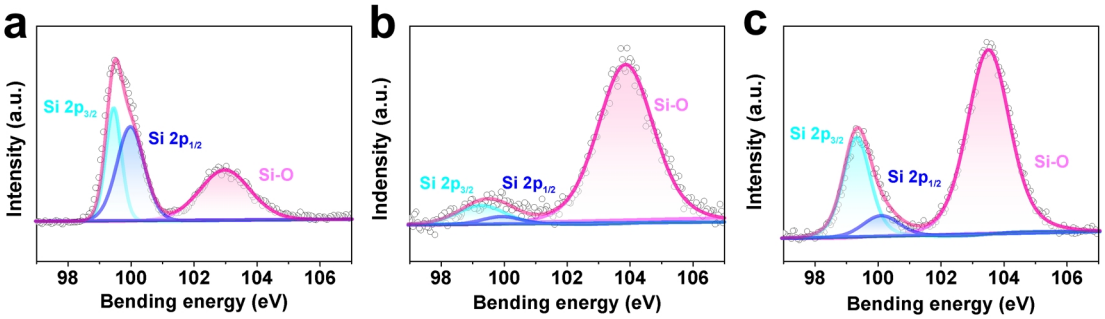

Figure S4. Si 2p spectrum of (a) Si NPs, (b) SSPB and (c) SSG.

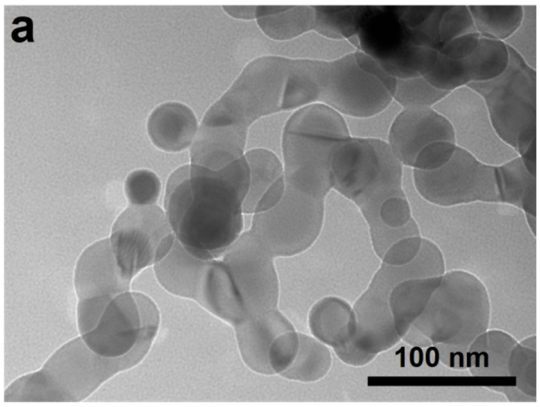

Figure S5. TEM image of Si NPs.

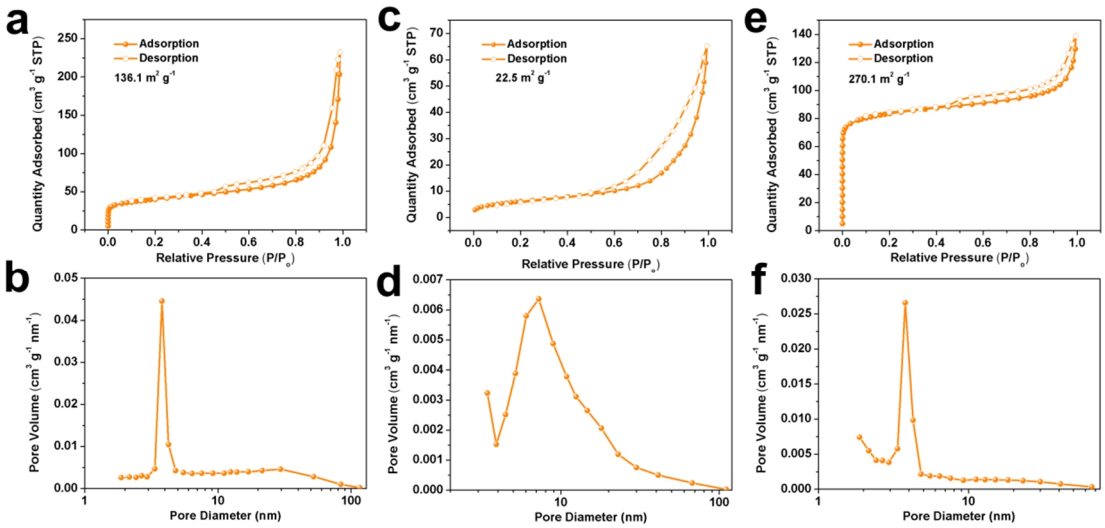

Figure S6. N_2 adsorption-desorption isotherms of (a) SSPBG, (c) SSG and (e) SSPB. Pore size distribution of (b) SSPBG, (d) SSG and (f) SSPB.

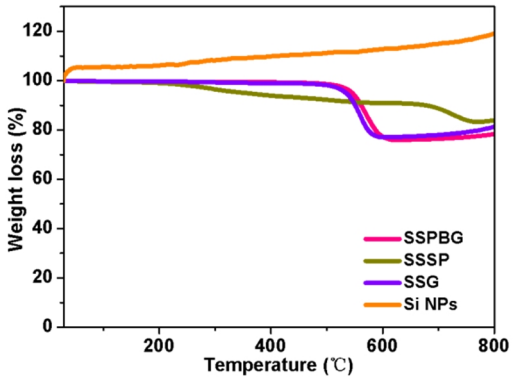

Figure S7. TGA curves of SSPBG and control electrodes obtained under 800 ℃ for 2 h at a heating rate of 10 ℃/min in air atmosphere.

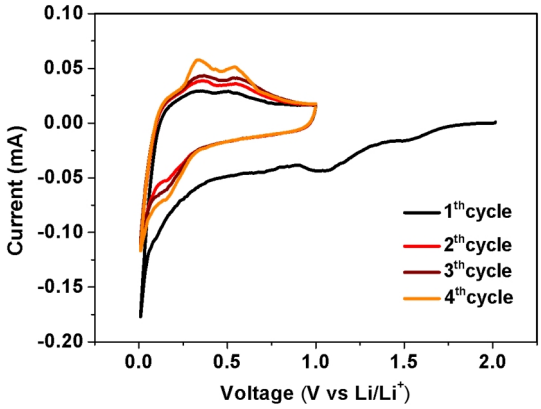

Figure S8. Typical CV curve of SSPBG.

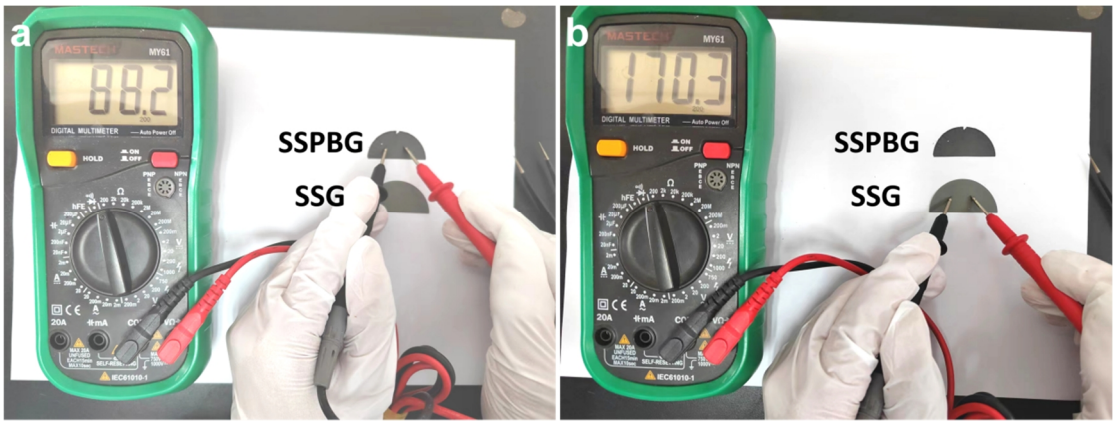

Figure S9. Photograph showing electrical conductivity of SSPBG (88.2 Ω) and SSG (170.3 Ω).

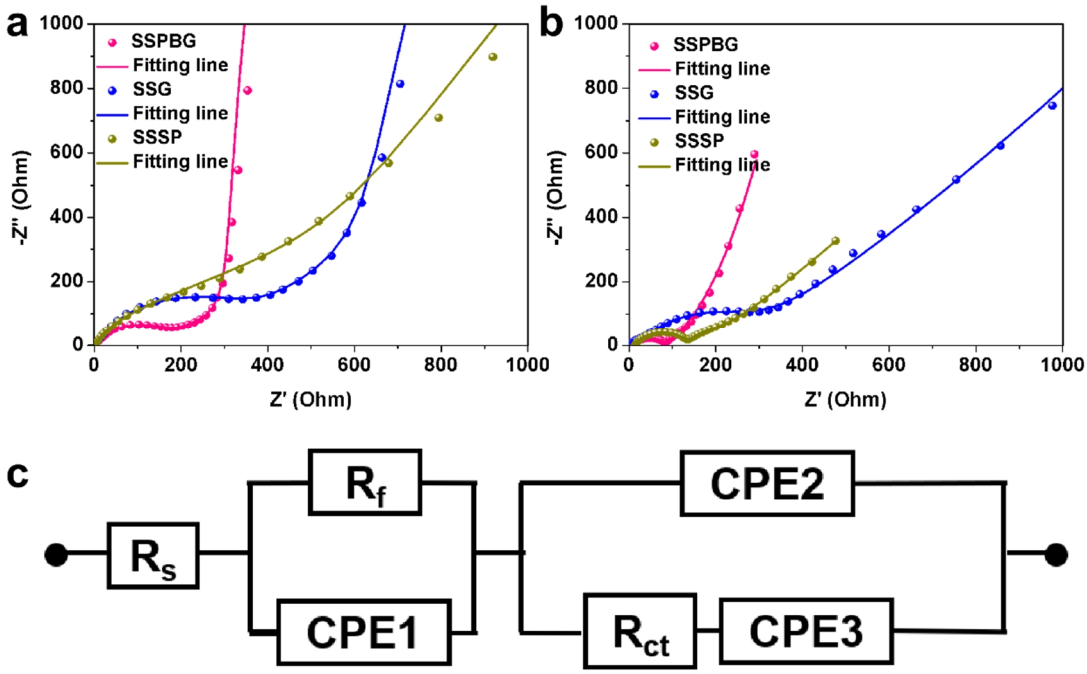

Figure S10. Nyquist plots of SSPBG, SSG and SSSP obtained from electrochemical impedance spectroscopy (EIS) measurement for (a) fresh electrodes and (b) electrodes after 100 cycles. (c) equivalent circuit.

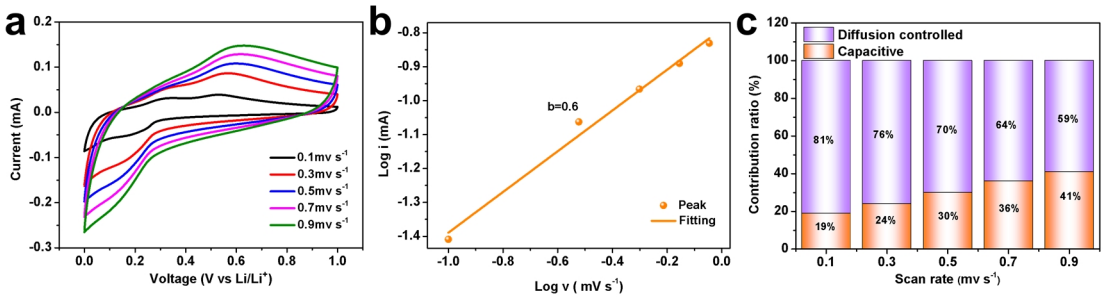

Figure S11. (a) CV curves of SSPBG electrodes at different scanning rates. (b) Relation between log(peak current) and log(scanning rate). (c) Contribution ratio of capacitive and diffusion-controlled charge storage at different scanning rates.

Table S1. Weight Distribution of Si in SSPBG, SSG and SSSP

	(%)	(630 ℃)	(770 ℃)	X_{Si} (%)
	W_{Si}	113	/	67
SSPBG	W_C	0	/	33
	W_{SSBG}	76	/	/
	W_{Si}	113	/	68
SSG	W_C	0	/	32
	W_{SG}	77.2	/	/
	W_{Si}	/	117	66
SSSP	W_C	/	0	34
	W_{SSSP}	/	78	/

Table S2. Fitted Electrochemical Impedance Value.

Sample	Rs/Ohm	Rf/Ohm	Rct/Ohm
SSPBG	2.119	122.3	381
SSG	1.67	1135	459
SSSP	2.236	211.9	1051
SSPBG after cycling	2.557	62.7	74.4
SSG after cycling	2.896	45.95	289.3
SSSP after cycling	12.67	413.3	181.8

Table S3. Literature on Self-supporting Si-based Anodes for Lithium-ion Batteries

Sample	Discharge capacity (mAh g^{-1})	Current density (mA g^{-1})	After n^{th} cycle	Ref.
CNTs/Si	1000	1000	50	[1]
CNTs/Si NPs	1510	840	100	[2]
PAN/Si/Ni	910	1000	100	[3]
Si NPs/porous carbon nanofifibers	870	100	100	[4]
Si NPs/carbon nanofifibers	869	400	480	[5]
Si NPs/graphene	1390	2000	200	[6]
Graphene/CNTs/Si	808	420	60	[7]
Si NPs/porous carbon/carbon black/CNTs	765	200	100	[8]
Si@SiO_2/bacterial cellulose/graphene	901	2000	500	This work

n REFERENCES

(1) Lin, H.; Weng, W.; Ren, J.; Qiu, L.; Zhang, Z.; Chen, P.; Chen, X.; Deng, J.; Wang, Y.; Peng, H. Twisted aligned carbon nanotube/silicon composite fiber anode for flexible wire-shaped lithium-ion battery. *Adv. Mater.* **2014**, 26, 1217-1222.

(2) Park, K. S.; Min, K. M.; Seo, S. D.; Lee, G. H.; Shim, H. W.; Kim, D. W. Self-supported multi-walled carbon nanotube-embedded silicon nanoparticle films for anodes of Li-ion batteries. *Mater. Res. Bull.* **2013**, 48, 1732-1736.

(3) Bao, W.; Wang, J.; Chen, S.; Li, W.; Su, Y.; Wu, F.; Tan, G.; Lu, J. A three-dimensional hierarchical structure of cyclized-PAN/Si/Ni for mechanically stable silicon anodes. *J. Mater. Chem. A* **2017**, 5, 24667-24676.

(4) Wang, M. S.; Song, W. L.; Wang, J.; Fan, L. Z. Highly uniform silicon nanoparticle/porous carbon nanofiber hybrids towards free-standing high-performance anodes for lithium-ion batteries. *Carbon* **2015**, 82, 337-345.

(5) Qu, E.; Chen, T.; Xiao, Q.; Lei, G.; Li, Z. Freestanding silicon/carbon nanofibers composite membrane as a flexible anode for Li-ion battery. *J. Power Sources* **2018**, 403, 103-108.

(6) Zhou, M.; Li, X.; Wang, B.; Zhang, Y.; Ning, J.; Xiao, Z.; Zhang, X.; Chang, Y.; Zhi, L. High-performance silicon battery anodes enabled by engineering graphene assemblies. *Nano Lett.* **2015**, 15, 6222-6228.

(7) Huang, Z. D.; Zhang, K.; Zhang, T. T.; Liu, R. Q.; Lin, X. J.; Li, Y.; Feng, X. M.; Mei, Q. B.; Masese, T.; Ma, Y. W.; Huang, W. Binder-free graphene/carbon nanotube/silicon hybrid grid as freestanding anode for high capacity lithium ion batteries. *Compos. Part A Appl. Sci. Manuf.* **2016**, 84, 386-392.

(8) Wu, J.; Qin, X.; Zhang, H.; He, Y. B.; Li, B.; Ke, L.; Lv, W.; Du, H.; Yang, Q. H.; Kang, F. Multilayered silicon embedded porous carbon/graphene hybrid film as a high performance anode. *Carbon* **2015**, 84, 434-443.